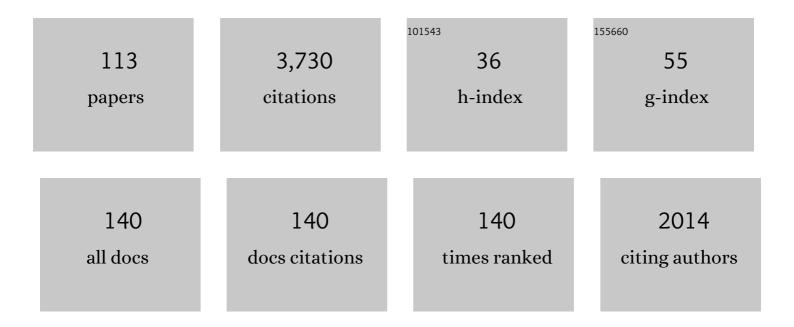
Stefan Markus Schmalholz

List of Publications by Year in descending order

Source: https://exaly.com/author-pdf/9443061/publications.pdf Version: 2024-02-01



#	Article	IF	CITATIONS
1	Melt Migration and Chemical Differentiation by Reactive Porosity Waves. Geochemistry, Geophysics, Geosystems, 2022, 23, .	2.5	4
2	Horizontal Force Required for Subduction Initiation at Passive Margins With Constraints From Slab Detachment. Frontiers in Earth Science, 2022, 10, .	1.8	3
3	A simple computer program for calculating stress and strain rate in 2D viscous inclusion-matrix systems. Journal of Structural Geology, 2022, 160, 104617.	2.3	3
4	Metamorphic Facies Distribution in the Western Alps Predicted by Petrologicalâ€Thermomechanical Models of Synâ€Convergent Exhumation. Geochemistry, Geophysics, Geosystems, 2022, 23, .	2.5	2
5	Peak Alpine metamorphic conditions from stauroliteâ€bearing metapelites in the Monte Rosa nappe (Central European Alps) and geodynamic implications. Journal of Metamorphic Geology, 2021, 39, 897-917.	3.4	7
6	Widening of Hydrous Shear Zones During Incipient Eclogitization of Metastable Dry and Rigid Lower Crust—HolsnÃ,y, Western Norway. Tectonics, 2021, 40, e2020TC006572.	2.8	21
7	On backflow associated with oceanic and continental subduction. Geophysical Journal International, 2021, 227, 576-590.	2.4	1
8	Buoyancy versus shear forces in building orogenic wedges. Solid Earth, 2021, 12, 1749-1775.	2.8	8
9	On exhumation velocities of high-pressure units based on insights from chemical zoning in garnet (Tianshan, NW China). Earth and Planetary Science Letters, 2021, 570, 117065.	4.4	13
10	Alpine peak pressure and tectono-metamorphic history of the Monte Rosa nappe: evidence from the cirque du Véraz, upper Ayas valley, Italy. Swiss Journal of Geosciences, 2021, 114, 20.	1.2	2
11	The importance of interfacial instability for viscous folding in mechanically heterogeneous layers. Geological Society Special Publication, 2020, 487, 45-58.	1.3	5
12	Quantification and visualization of finite strain in 3D viscous numerical models of folding and overthrusting. Journal of Structural Geology, 2020, 131, 103945.	2.3	4
13	2D Hydroâ€Mechanicalâ€Chemical Modeling of (De)hydration Reactions in Deforming Heterogeneous Rock: The Periclaseâ€Brucite Model Reaction. Geochemistry, Geophysics, Geosystems, 2020, 21, e2020GC009351.	2.5	20
14	Contributions of Grain Damage, Thermal Weakening, and Necking to Slab Detachment. Frontiers in Earth Science, 2020, 8, .	1.8	8
15	Interaction of folding and thrusting during fold-and-thrust-belt evolution: Insights from numerical simulations and application to the Swiss Jura and the Canadian Foothills. Tectonophysics, 2020, 789, 228474.	2.2	8
16	Impact of crust–mantle mechanical coupling on the topographic and thermal evolutions during the necking phase of â€~magma-poor' and â€~sediment-starved' rift systems: A numerical modeling study. Tectonophysics, 2020, 786, 228472.	2.2	16
17	A case of Ampferer-type subduction and consequences for the Alps and the Pyrenees. Numerische Mathematik, 2020, 320, 313-372.	1.4	40
18	Stress and deformation mechanisms at a subduction zone: insights from 2-D thermomechanical numerical modelling. Geophysical Journal International, 2020, 221, 1605-1625.	2.4	24

#	Article	IF	CITATIONS
19	Thermal softening induced subduction initiation at a passive margin. Geophysical Journal International, 2020, 220, 2068-2073.	2.4	23
20	Tectonic inheritance controls nappe detachment, transport and stacking in the Helvetic nappe system, Switzerland: insights from thermomechanical simulations. Solid Earth, 2020, 11, 287-305.	2.8	7
21	Impact of upper mantle convection on lithosphere hyperextension and subsequent horizontally forced subduction initiation. Solid Earth, 2020, 11, 2327-2357.	2.8	7
22	Control of 3-D tectonic inheritance on fold-and-thrust belts: insights from 3-D numerical models and application to the Helvetic nappe system. Solid Earth, 2020, 11, 999-1026.	2.8	8
23	Relation between mean stress, thermodynamic, and lithostatic pressure. Journal of Metamorphic Geology, 2019, 37, 1-14.	3.4	40
24	Emersion of Distal Domains in Advanced Stages of Continental Rifting Explained by Asynchronous Crust and Mantle Necking. Geochemistry, Geophysics, Geosystems, 2019, 20, 3821-3840.	2.5	23
25	Metamorphic pressure variation in a coherent Alpine nappe challenges lithostatic pressure paradigm. Nature Communications, 2019, 10, 4734.	12.8	42
26	Spontaneous generation of ductile shear zones by thermal softening: Localization criterion, 1D to 3D modelling and application to the lithosphere. Earth and Planetary Science Letters, 2019, 519, 284-296.	4.4	32
27	Thinning mechanisms of heterogeneous continental lithosphere. Earth and Planetary Science Letters, 2019, 512, 147-162.	4.4	44
28	Resolving thermomechanical coupling in two and three dimensions: spontaneous strain localization owing to shear heating. Geophysical Journal International, 2019, 216, 365-379.	2.4	23
29	Distribution and magnitude of stress due to lateral variation of gravitational potential energy between Indian lowland and Tibetan plateau. Geophysical Journal International, 2019, 216, 1313-1333.	2.4	25
30	Spontaneous ductile crustal shear zone formation by thermal softening and related stress, temperature and strain rate evolution. Tectonophysics, 2018, 746, 384-397.	2.2	19
31	Formation of orogenic wedges and crustal shear zones by thermal softening, associated topographic evolution and application to natural orogens. Tectonophysics, 2018, 746, 512-529.	2.2	24
32	High Pressure Metamorphism Caused by Fluid Induced Weakening of Deep Continental Crust. Scientific Reports, 2018, 8, 17011.	3.3	44
33	Necking of the Lithosphere: A Reappraisal of Basic Concepts With Thermoâ€Mechanical Numerical Modeling. Journal of Geophysical Research: Solid Earth, 2018, 123, 5279-5299.	3.4	27
34	Spatial relation of surface faults and crustal seismicity: a first comparison in the region of Switzerland. Acta Geodaetica Et Geophysica, 2018, 53, 439-461.	1.6	11
35	M2Di: Concise and efficient <scp>MATLAB</scp> 2â€Ð <scp>S</scp> tokes solvers using the Finite Difference Method. Geochemistry, Geophysics, Geosystems, 2017, 18, 755-768.	2.5	19
36	Tectonic inheritance and kinematic strain localization as trigger for the formation of the Helvetic nappes, Switzerland. Swiss Journal of Geosciences, 2017, 110, 523-534.	1.2	8

#	Article	IF	CITATIONS
37	Impact of grain size evolution on necking in calcite layers deforming by combined diffusion and dislocation creep. Journal of Structural Geology, 2017, 103, 37-56.	2.3	15
38	Folding and necking across the scales: a review of theoretical and experimental results and their applications. Solid Earth, 2016, 7, 1417-1465.	2.8	47
39	3-D numerical models of viscous flow applied to fold nappes and the Rawil depression in the Helvetic nappe system (western Switzerland). Journal of Structural Geology, 2016, 86, 32-46.	2.3	26
40	Nonlithostatic pressure during subduction and collision and the formation of (ultra)high-pressure rocks. Geology, 2016, 44, 343-346.	4.4	45
41	Exhumation of the Dora Maira ultrahighâ€pressure unit by buoyant uprise within a lowâ€viscosity mantle obliqueâ€slip shear zone. Terra Nova, 2016, 28, 348-355.	2.1	11
42	Dramatic effect of elasticity on thermal softening and strain localization during lithospheric shortening. Geophysical Journal International, 2016, 204, 780-784.	2.4	18
43	A 3â€Ð Lagrangian finite element algorithm with remeshing for simulating largeâ€strain hydrodynamic instabilities in power law viscoelastic fluids. Geochemistry, Geophysics, Geosystems, 2015, 16, 215-245.	2.5	7
44	Shear zone and nappe formation by thermal softening, related stress and temperature evolution, and application to the Alps. Journal of Metamorphic Geology, 2015, 33, 887-908.	3.4	27
45	Current challenges for explaining (ultra)highâ€pressure tectonism in the Pennine domain of the Central and Western Alps. Journal of Metamorphic Geology, 2015, 33, 869-886.	3.4	32
46	Transition from thin- to thick-skinned tectonics and consequences for nappe formation: Numerical simulations and applications to the Helvetic nappe system, Switzerland. Tectonophysics, 2015, 665, 101-117.	2.2	26
47	A dimensional analysis to quantify the thermal budget around lithosphericâ€scale shear zones. Terra Nova, 2015, 27, 163-168.	2.1	15
48	From symmetric necking to localized asymmetric shearing: The role of mechanical layering. Geology, 2015, 43, 711-714.	4.4	12
49	Relationship between tectonic overpressure, deviatoric stress, driving force, isostasy and gravitational potential energy. Geophysical Journal International, 2014, 197, 680-696.	2.4	80
50	Quantifying the impact of mechanical layering and underthrusting on the dynamics of the modern Indiaâ€Asia collisional system with 3â€D numerical models. Journal of Geophysical Research: Solid Earth, 2014, 119, 616-644.	3.4	18
51	Metamorphism under stress: The problem of relating minerals to depth. Geology, 2014, 42, 733-734.	4.4	36
52	Physicsâ€controlled thickness of shear zones caused by viscous heating: Implications for crustal shear localization. Geophysical Research Letters, 2014, 41, 4904-4911.	4.0	39
53	Viscous overthrusting versus folding: 2-D quantitative modeling and its application to the Helvetic and Jura fold and thrust belts. Journal of Structural Geology, 2014, 62, 25-37.	2.3	15
54	Wave propagation in unsaturated porous media. Acta Mechanica, 2014, 225, 2435-2448.	2.1	26

#	Article	IF	CITATIONS
55	Kinematics and dynamics of tectonic nappes: 2-D numerical modelling and implications for high and ultra-high pressure tectonism in the Western Alps. Tectonophysics, 2014, 631, 160-175.	2.2	47
56	Numerical simulation of ambient seismic wavefield modification caused by pore-fluid effects in an oil reservoir. Geophysics, 2013, 78, T41-T52.	2.6	14
57	A simple thermo-mechanical shear model applied to the Morcles fold nappe (Western Alps). Tectonophysics, 2013, 583, 76-87.	2.2	14
58	Thermo-mechanical model for the finite strain gradient in kilometer-scale shear zones. Geology, 2013, 41, 567-570.	4.4	6
59	Tectonic overpressure in weak crustalâ€scale shear zones and implications for the exhumation of highâ€pressure rocks. Geophysical Research Letters, 2013, 40, 1984-1988.	4.0	110
60	Folding in power-law viscous multi-layers. Philosophical Transactions Series A, Mathematical, Physical, and Engineering Sciences, 2012, 370, 1798-1826.	3.4	51
61	Pore fluid effects on S-wave attenuation caused by wave-induced fluid flow. Geophysics, 2012, 77, L13-L23.	2.6	55
62	Phase Velocity Dispersion and Attenuation of Seismic Waves due to Trapped Fluids in Residual Saturated Porous Media. Vadose Zone Journal, 2012, 11, vzj2011.0121.	2.2	28
63	Lateral fold growth and fold linkage. Geology, 2012, 40, 1039-1042.	4.4	38
64	Pinch-and-swell structure and shear zones in viscoplastic layers. Journal of Structural Geology, 2012, 37, 75-88.	2.3	49
65	Quasi-static finite element modeling of seismic attenuation and dispersion due to wave-induced fluid flow in poroelastic media. Journal of Geophysical Research, 2011, 116, .	3.3	148
66	A simple analytical solution for slab detachment. Earth and Planetary Science Letters, 2011, 304, 45-54.	4.4	38
67	Time-reverse imaging with limited S-wave velocity model information. Geophysics, 2011, 76, MA33-MA40.	2.6	8
68	The exponential flow law applied to necking and folding of a ductile layer. Geophysical Journal International, 2011, 184, 83-89.	2.4	37
69	Comparing thin-sheet models with 3-D multilayer models for continental collision. Geophysical Journal International, 2011, 187, 10-33.	2.4	33
70	Thermo-Tectono-Stratigraphic Forward Modelling of the Upper Rhine Graben in reference to geometric balancing: Brittle crustal extension on a highly viscous mantle. Tectonophysics, 2011, 509, 1-13.	2.2	10
71	Spectral analysis of ambient ground-motion—Noise reduction techniques and a methodology for mapping horizontal inhomogeneity. Journal of Applied Geophysics, 2011, 74, 100-113.	2.1	10
72	Impact of fluid saturation on the reflection coefficient of a poroelastic layer. Geophysics, 2011, 76, N1-N12.	2.6	44

#	Article	IF	CITATIONS
73	Sâ€wave attenuation caused by waveâ€induced fluid flow. , 2011, , .		Ο
74	S-wave attenuation caused by wave-induced fluid flow. , 2011, , .		0
75	Finite element modeling of seismic attenuation due to fluid flow in partially saturated rocks. , 2010, , .		Ο
76	Comment on â€~Folding with thermal-mechanical feedback'. Journal of Structural Geology, 2010, 32, 127-130.	2.3	13
77	Kinematics of constant arc length folding for different fold shapes. Journal of Structural Geology, 2010, 32, 755-765.	2.3	17
78	Dynamic unfolding of multilayers: 2D numerical approach and application to turbidites in SW Portugal. Tectonophysics, 2010, 494, 64-74.	2.2	10
79	Reply to comment on â€~Lowâ€frequency microtremor anomalies at an oil and gas field in Voitsdorf, Austria' by Marcâ€André Lambert, Stefan M. Schmalholz, Erik H. Saenger and Brian Steiner, <i>Geophysical Prospecting</i> 57, 393–411. Geophysical Prospecting, 2010, 58, 341-346.	1.9	4
80	Finite-element simulations of Stoneley guided-wave reflection and scattering at the tips of fluid-filled fractures. Geophysics, 2010, 75, T23-T36.	2.6	59
81	Stress orientation and fracturing during three-dimensional buckling: Numerical simulation and application to chocolate-tablet structures in folded turbidites, SW Portugal. Tectonophysics, 2010, 493, 187-195.	2.2	29
82	Spectral modification of seismic waves propagating through solids exhibiting a resonance frequency: a 1-D coupled wave propagation-oscillation model. Geophysical Journal International, 2009, 176, 589-600.	2.4	41
83	Lowâ€frequency microtremor anomalies at an oil and gas field in Voitsdorf, Austria. Geophysical Prospecting, 2009, 57, 393-411.	1.9	50
84	A passive seismic survey over a gas field: Analysis of low-frequency anomalies. Geophysics, 2009, 74, O29-O40.	2.6	80
85	Low-frequency reflections from a thin layer with high attenuation caused by interlayer flow. Geophysics, 2009, 74, N15-N23.	2.6	77
86	Stress-strength relationship in the lithosphere during continental collision. Geology, 2009, 37, 775-778.	4.4	50
87	"Low-frequency reflections from a thin layer with high attenuation caused by interlayer flow,― GEOPHYSICS, 74, no. 1, N15–N23. Geophysics, 2009, 74, Y7-Y7.	2.6	1
88	Conceptual model of hydrocarbon reservoir related microtremors. , 2009, , .		2
89	Using spectral attributes to detect seismic tremor sources $\hat{a} {\in} "$ a synthetic study. , 2009, , .		0
90	Frequencyâ€dependent reflections from a layer with attenuation caused by interlayer flow. , 2009, , .		1

#	Article	IF	CITATIONS
91	Evolution of pinch-and-swell structures in a power-law layer. Journal of Structural Geology, 2008, 30, 649-663.	2.3	65
92	Numerical modelling of the effect of matrix anisotropy orientation on single layer fold development. Journal of Structural Geology, 2008, 30, 1013-1023.	2.3	16
93	Time reverse modeling of lowâ€frequency microtremors: Application to hydrocarbon reservoir localization. Geophysical Research Letters, 2008, 35, .	4.0	92
94	A benchmark comparison of spontaneous subduction models—Towards a free surface. Physics of the Earth and Planetary Interiors, 2008, 171, 198-223.	1.9	361
95	Comparison of finite difference and finite element methods for simulating two-dimensional scattering of elastic waves. Physics of the Earth and Planetary Interiors, 2008, 171, 112-121.	1.9	48
96	3D numerical modeling of forward folding and reverse unfolding of a viscous single-layer: Implications for the formation of folds and fold patterns. Tectonophysics, 2008, 446, 31-41.	2.2	47
97	Viscous heating allows thrusting to overcome crustal-scale buckling: Numerical investigation with application to the Himalayan syntaxes. Earth and Planetary Science Letters, 2008, 274, 189-203.	4.4	84
98	Automated thermotectonostratigraphic basin reconstruction: Viking Graben case study. AAPG Bulletin, 2008, 92, 309-326.	1.5	38
99	Finite-difference modeling of wave propagation on microscale: A snapshot of the work in progress. Geophysics, 2007, 72, SM293-SM300.	2.6	43
100	Seismic lowâ€frequency anomalies in multiple reflections from thinly layered poroelastic reservoirs. , 2007, , .		13
101	Lowâ€frequency anomalies in spectral ratios of singleâ€station microtremor measurements: Observations across an oil and gas field in Austria. , 2007, , .		14
102	3D finite amplitude folding: Implications for stress evolution during crustal and lithospheric deformation. Geophysical Research Letters, 2006, 33, .	4.0	72
103	Scaled amplification equation: A key to the folding history of buckled viscous single-layers. Tectonophysics, 2006, 419, 41-53.	2.2	40
104	Impact of mechanical anisotropy and power-law rheology on single layer folding. Tectonophysics, 2006, 421, 71-87.	2.2	23
105	Numerical simulations of parasitic folding in multilayers. Journal of Structural Geology, 2006, 28, 1647-1657.	2.3	58
106	Structural softening of the lithosphere. Terra Nova, 2005, 17, 66-72.	2.1	32
107	Effect of mineral phase transitions on sedimentary basin subsidence and uplift. Earth and Planetary Science Letters, 2005, 233, 213-228.	4.4	93
108	Viscoelastic folding: Maxwell versus Kelvin Rheology. Geophysical Research Letters, 2001, 28, 1835-1838.	4.0	18

#	Article	IF	CITATIONS
109	Strain and competence contrast estimation from fold shape. Tectonophysics, 2001, 340, 195-213.	2.2	58
110	A spectral/finite difference method for simulating large deformations of heterogeneous, viscoelastic materials. Geophysical Journal International, 2001, 145, 199-208.	2.4	69
111	Finite amplitude folding: transition from exponential to layer length controlled growth. Earth and Planetary Science Letters, 2000, 179, 363-377.	4.4	30
112	Finite amplitude folding: transition from exponential to layer length controlled growth. Earth and Planetary Science Letters, 2000, 181, 619-633.	4.4	28
113	Buckling versus folding: Importance of viscoelasticity. Geophysical Research Letters, 1999, 26, 2641-2644.	4.0	90